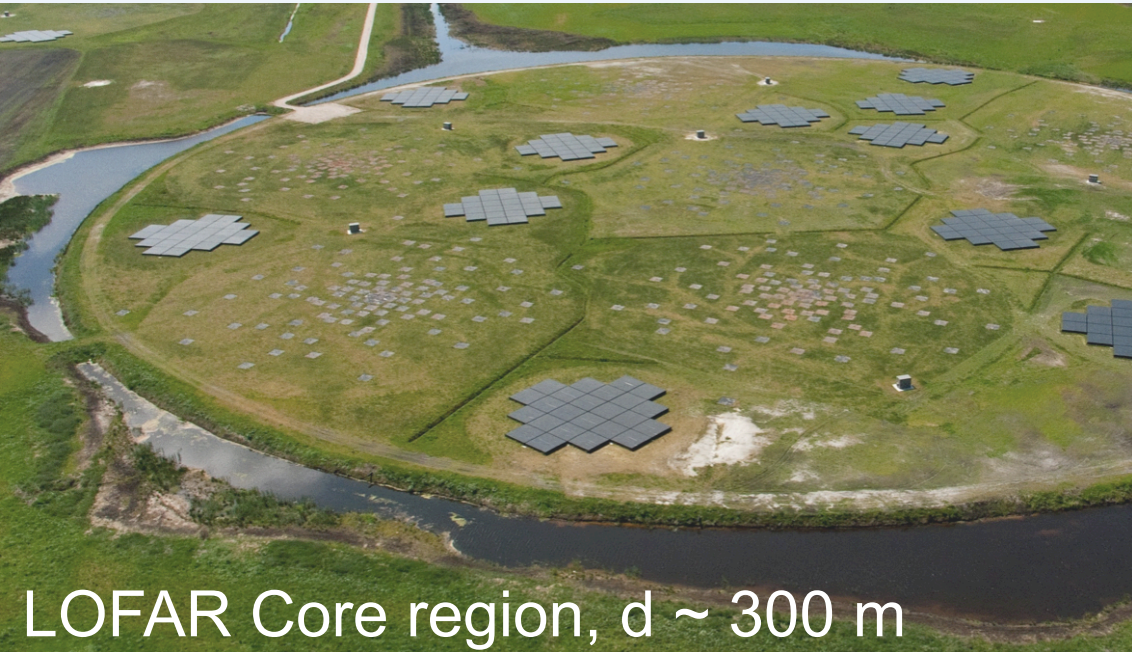
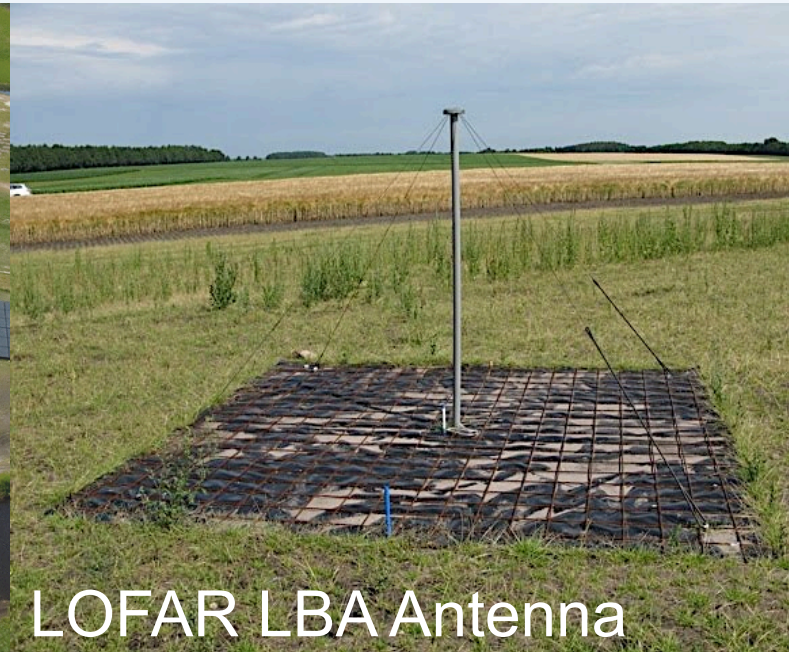


# Polarized radio emission and radio wavefront shape of extensive air showers



LOFAR Core region,  $d \sim 300$  m



LOFAR LBA Antenna

Arthur Corstanje

Radboud University Nijmegen

for the LOFAR Key Science Project Cosmic Rays

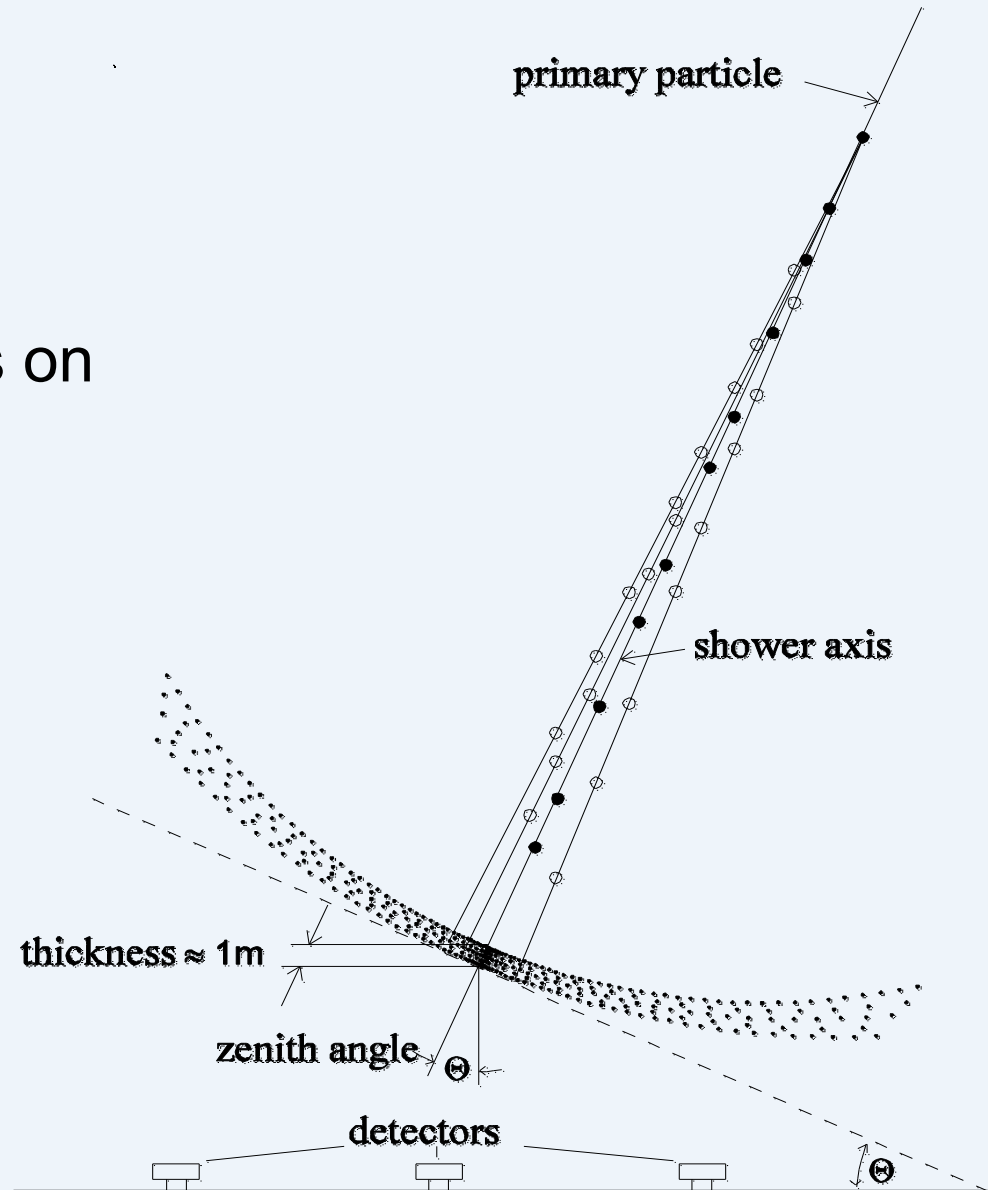
PoS (ICRC2015) 396

# Radio pulses from air showers

Short ( $\sim 10$  to  $100$  ns) pulses from extensive air showers, primary energy  $> \sim 10^{17}$  eV

In 200 - 400 LOFAR antennas on the ground, we measure:

- Lateral distribution of
  - Signal power
  - Signal arrival time
    - Wavefront shape
  - Polarization
  - Spectrum / pulse shape



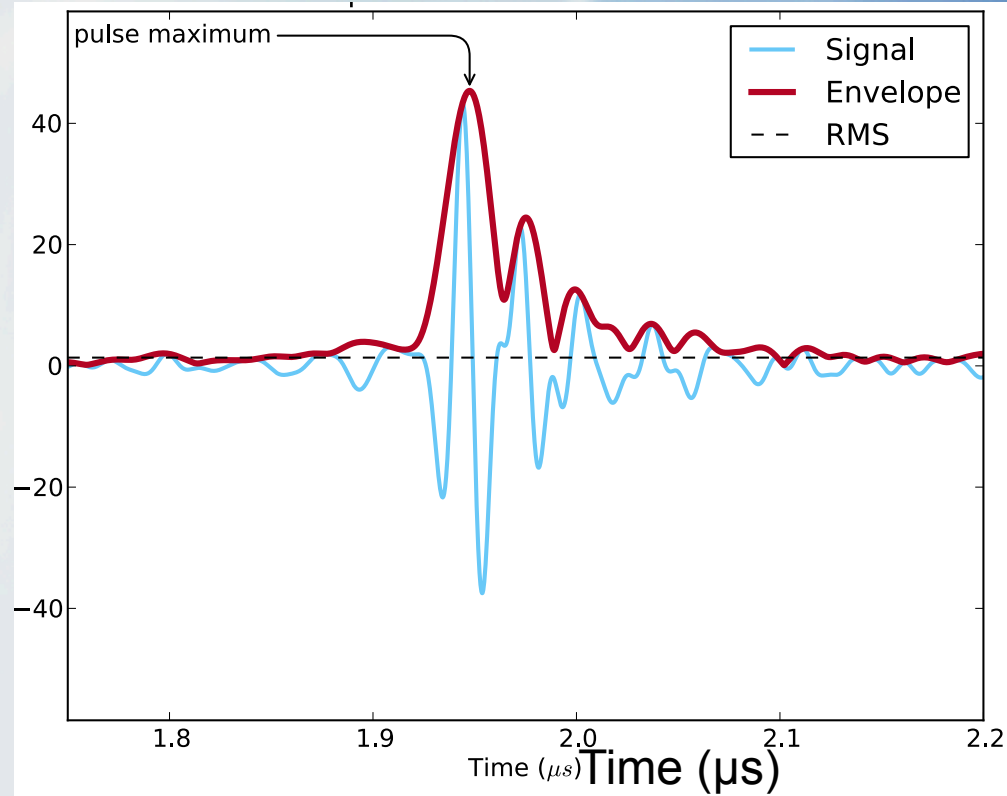
# Arrival times for the radio signal

Measuring arrival time of pulse in individual antennas:

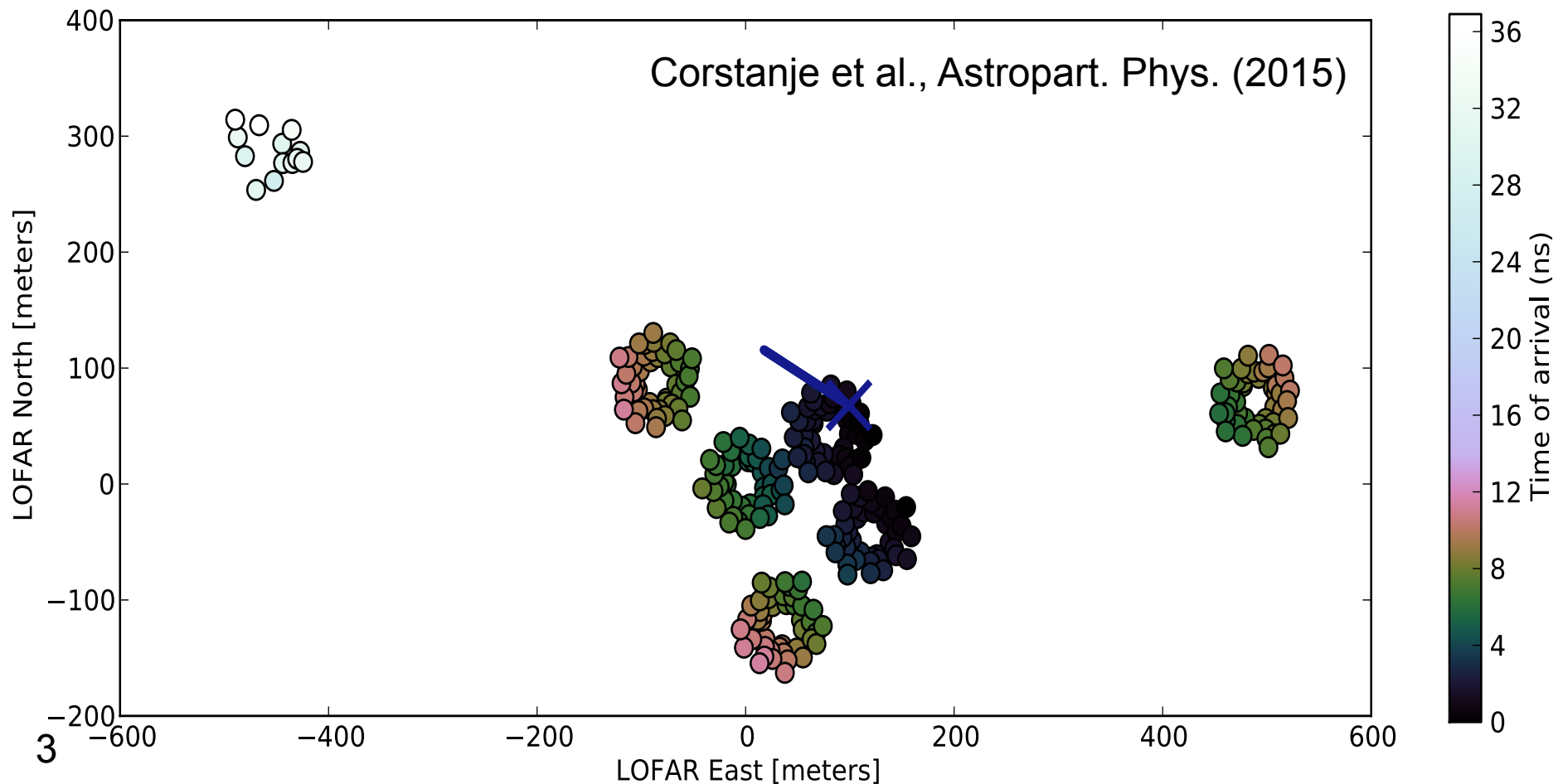
- Time series signal  
Apply Hilbert transform to get *Hilbert envelope*
- Define envelope maximum as 'the arrival time'

$$\sigma_t = \frac{12.7}{SNR} \text{ ns} < 5 \text{ ns!}$$

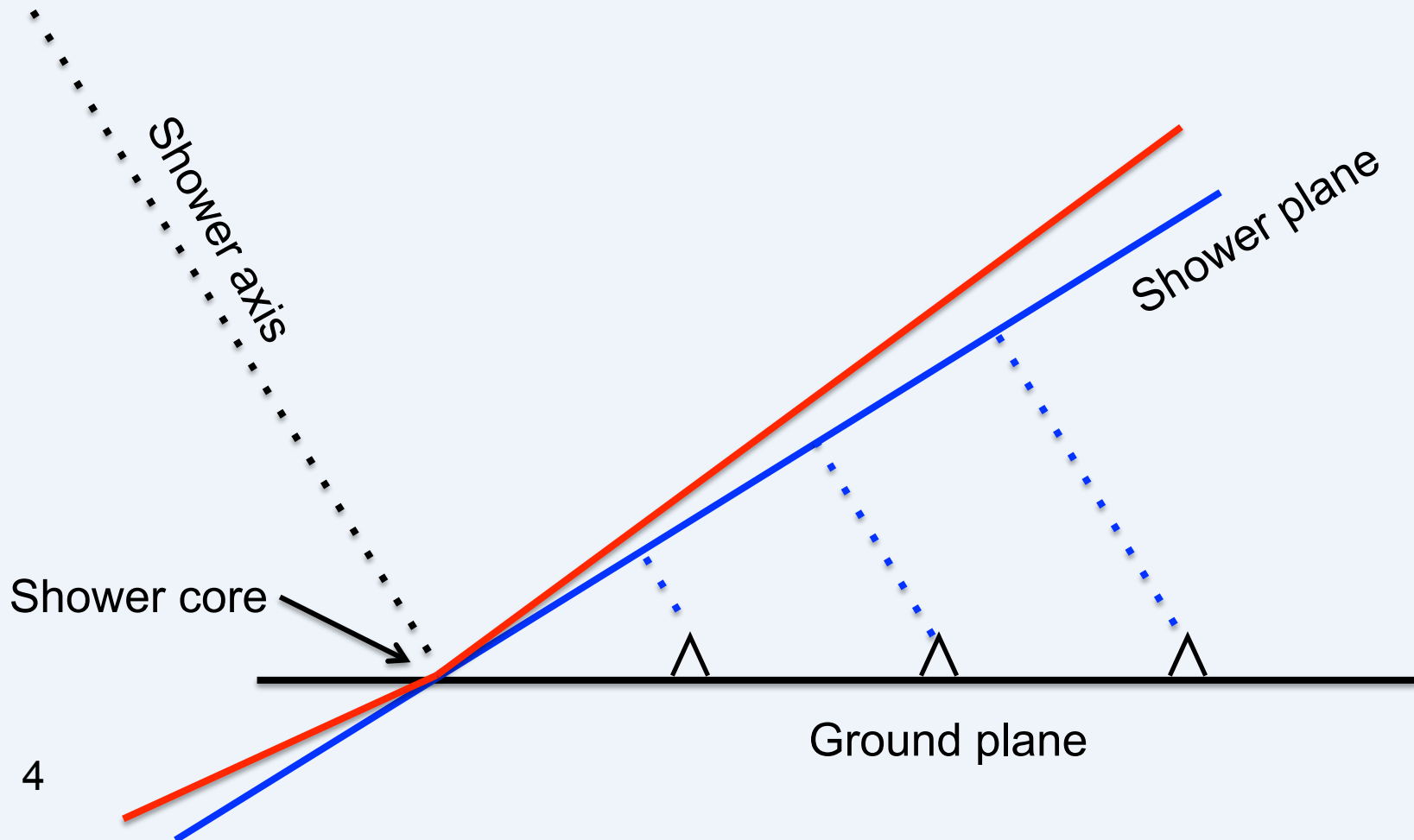
Amplitude



# Arrival times after subtracting plane-wave solution



# Shower plane projection



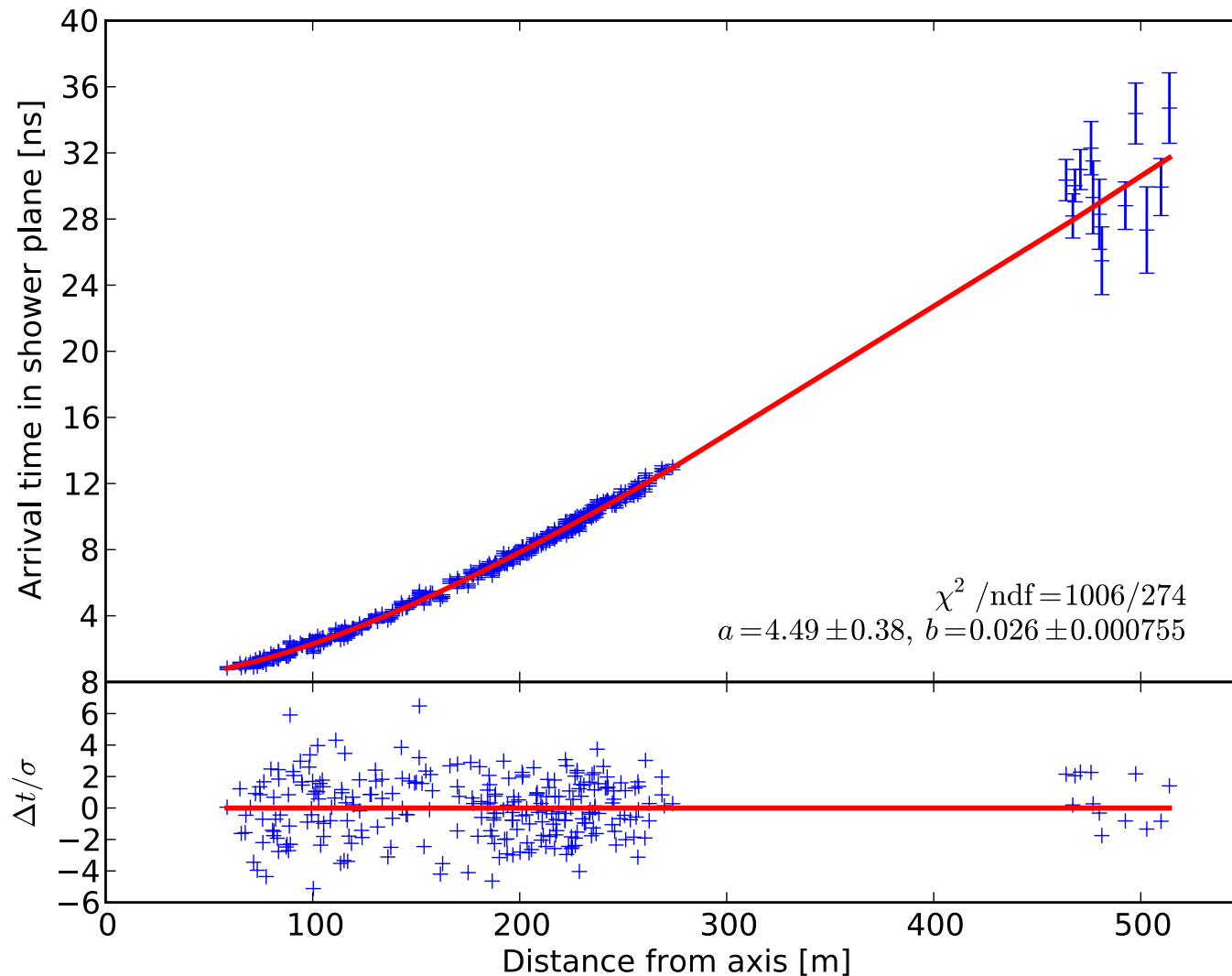


# Wavefront in the shower plane

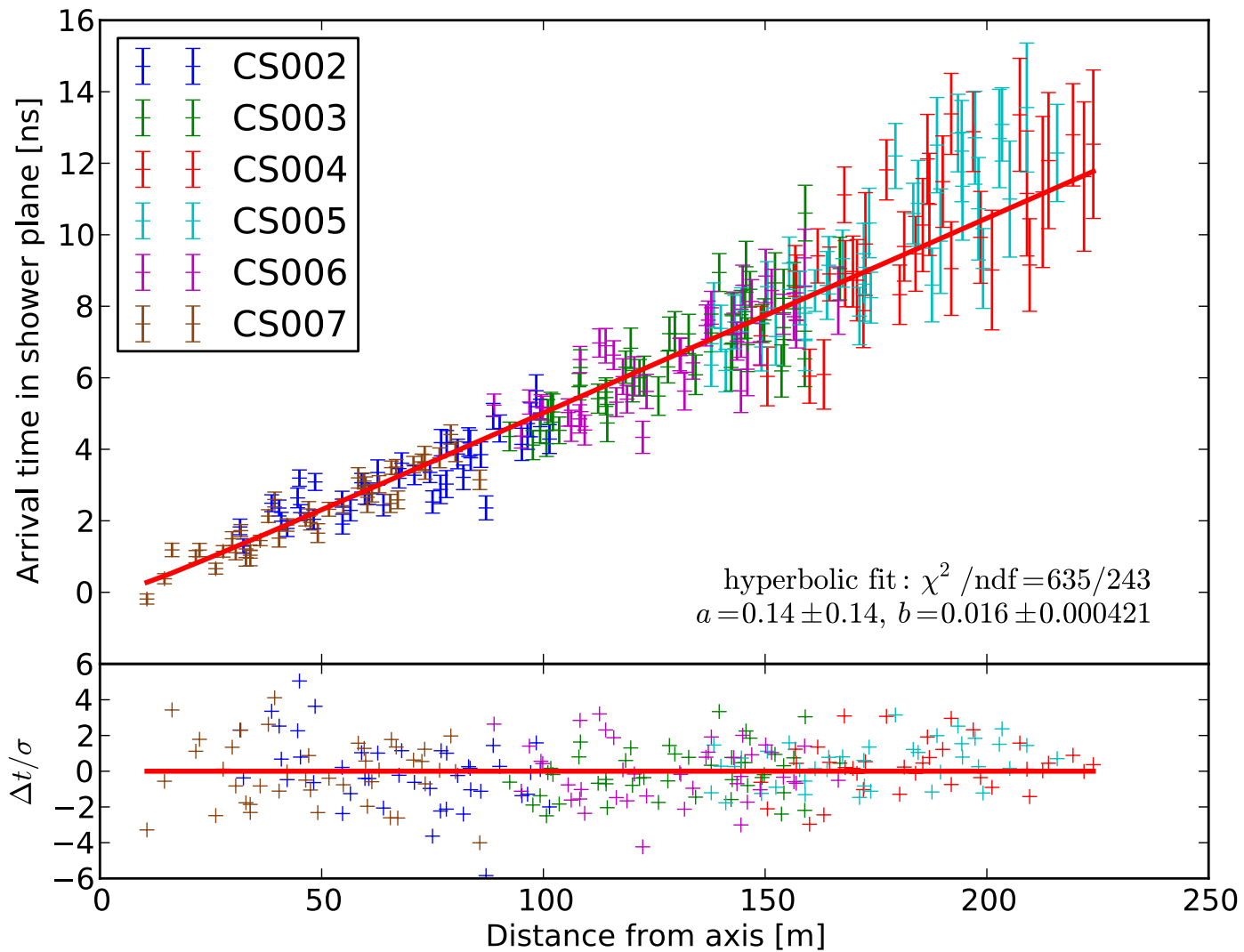
- Project antennas into shower plane
  - Shower axis position: fixed using power-LDF
  - Shower axis direction unknown to desired accuracy: **free fit parameters**
- Wavefront: arrival times as function of distance from shower axis
- Nested fitting (**5** parameters):
  - Optimize shower axis **direction** (2)
    - Optimize **curve-fit** (3)

# Best-fitting hyperbolic shape

Corstanje et al., Astropart. Phys. (2015)



# Conical-shaped example

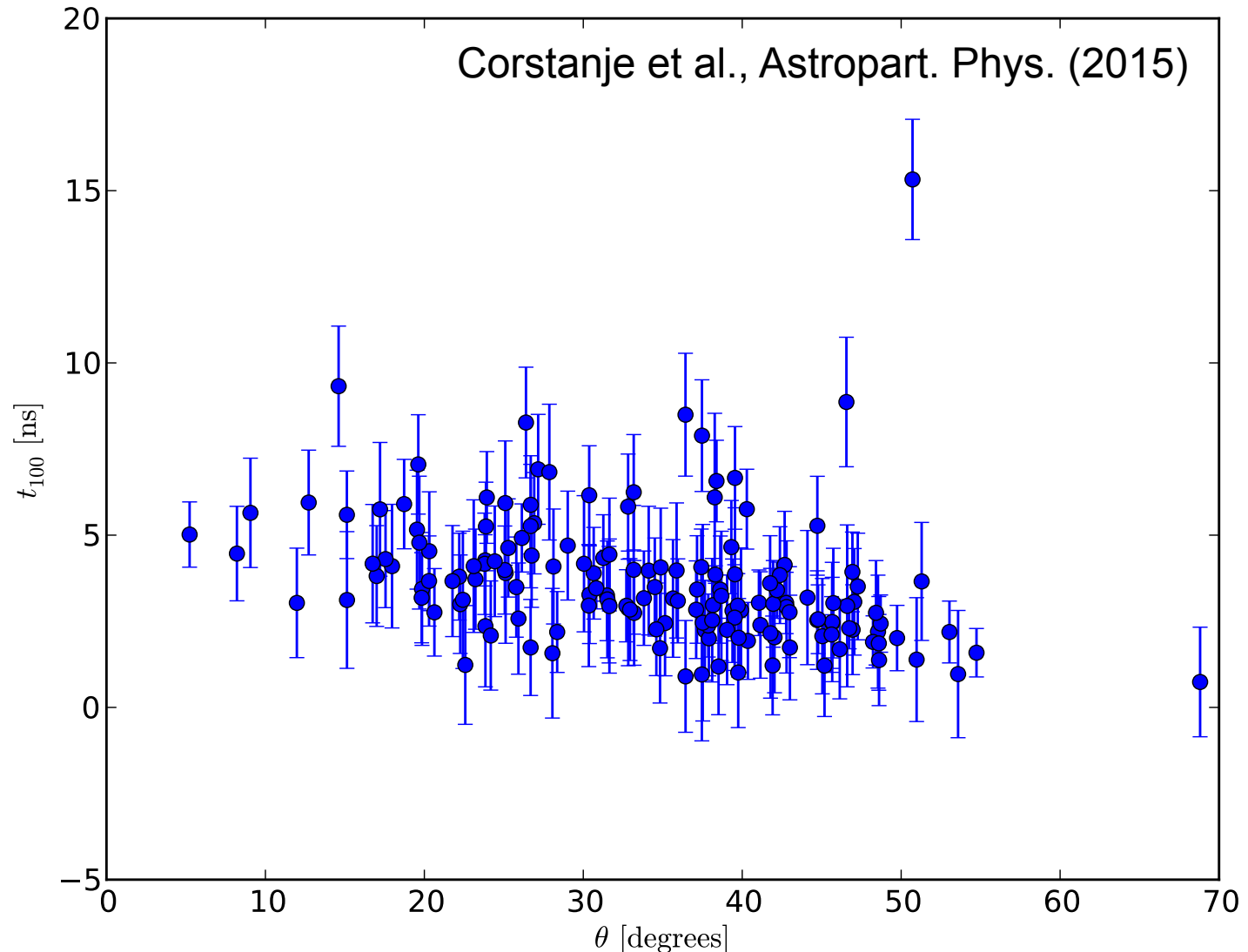




# Correlation with zenith angle

Time lag at  
100 m from  
shower core

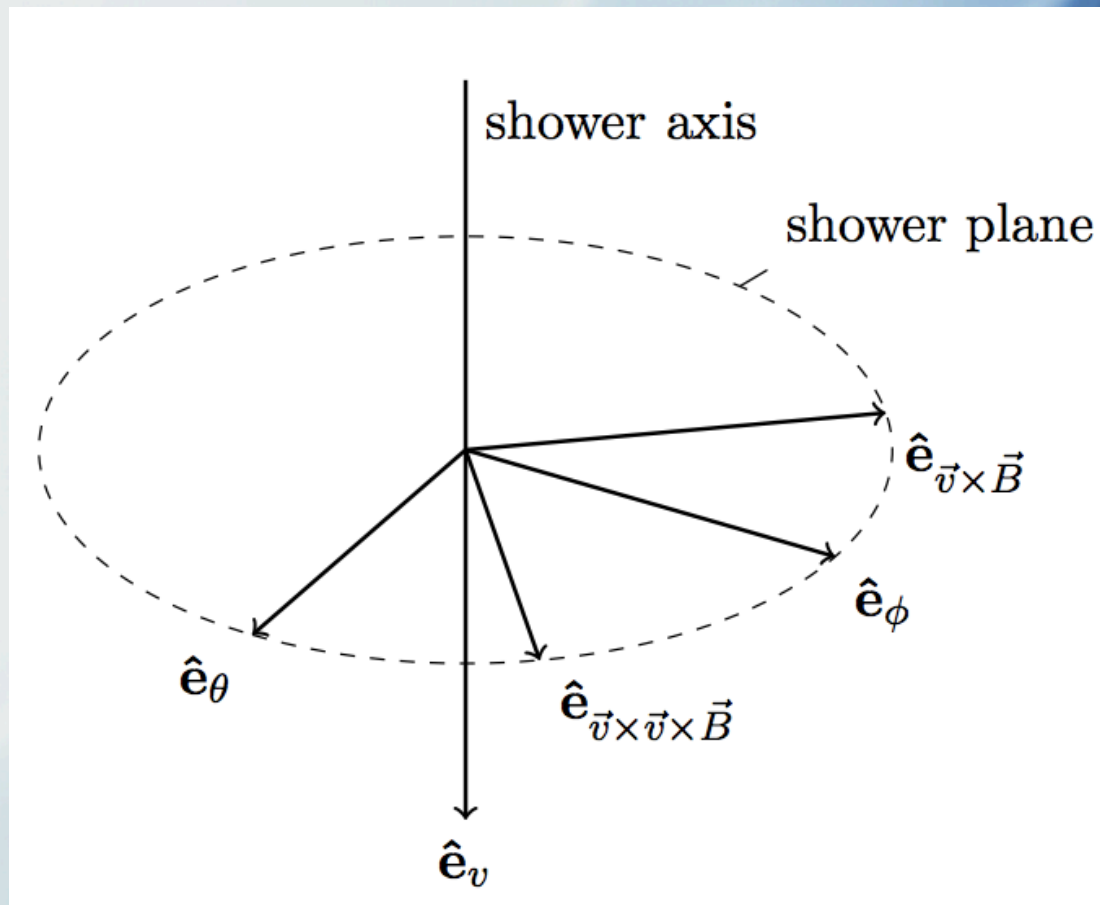
Decreases  
with zenith  
angle



# Polarization measurements

- Each LOFAR antenna offers two polarizations (NE-SW and NW-SE)
- Projected to 'on-sky' polarization when accounting for antenna model (Jones matrix)
- Polarizations further rotated to align with  $\vec{v} \times \vec{B}$  and  $\vec{v} \times (\vec{v} \times \vec{B})$ ,  
 $\vec{v}$  is shower axis  
 $\vec{B}$  is magnetic field

Schellart et al., JCAP (2014)



# Radio emission mechanisms

- Geomagnetic contribution,  
electric field aligned to  $\vec{v} \times \vec{B}$ :  $\vec{E}_G(\vec{r}) = E_G \hat{\vec{e}}_{\vec{v} \times \vec{B}}$
- Charge-excess contribution: electric field radially outward from shower core:

$$\vec{E}_C(\vec{r}) = E_C \cos \phi \hat{\vec{e}}_{\vec{v} \times \vec{B}} + E_C \sin \phi \hat{\vec{e}}_{\vec{v} \times (\vec{v} \times \vec{B})}$$

- Assuming these contributions account for total E-field
- Charge-excess fraction:  $a(\vec{r}) = \frac{E_C}{E_G} \sin \alpha$

where  $\alpha$  is angle of magnetic field with shower axis

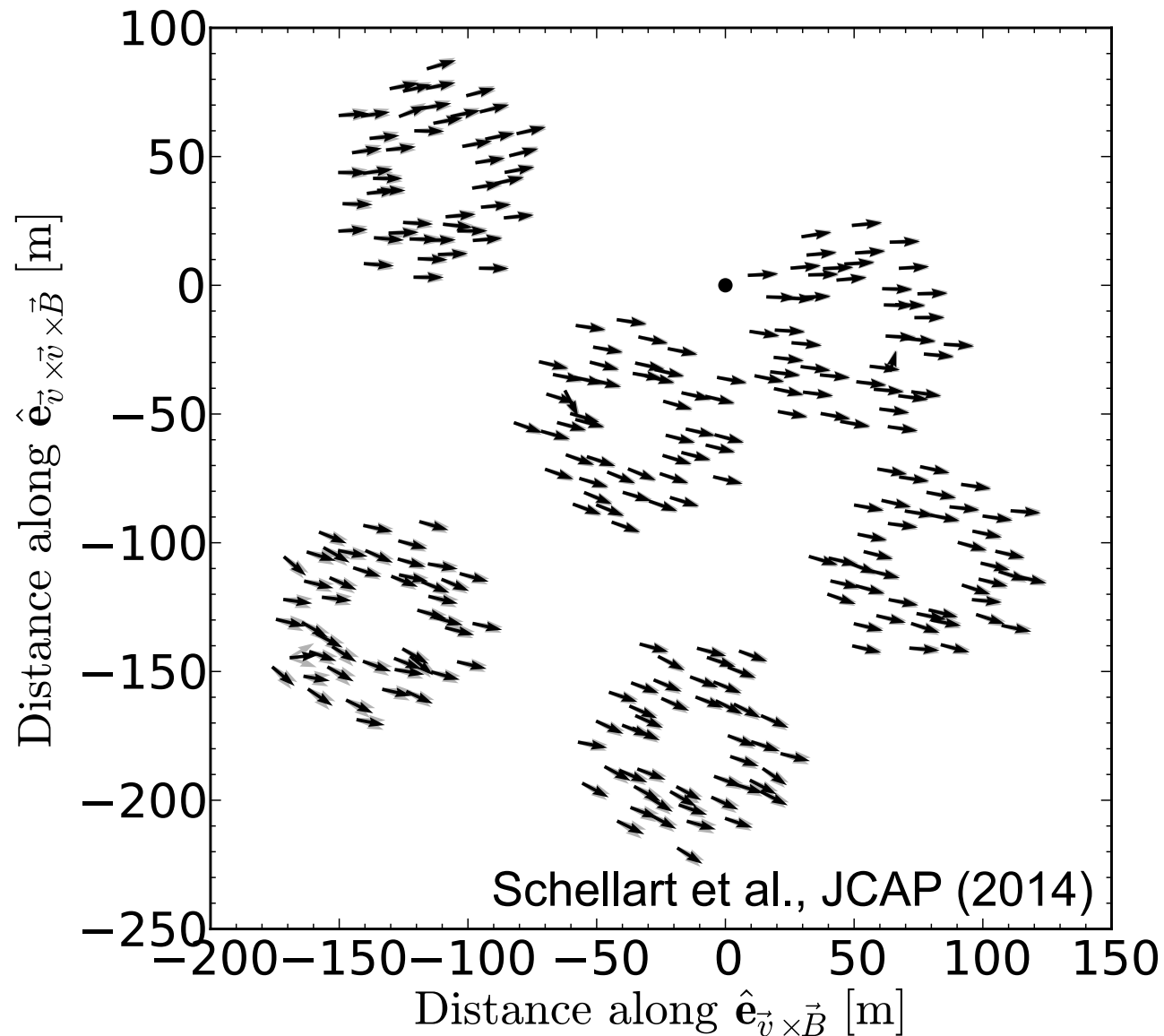
# Example polarization footprint

Mostly parallel to  
the  $\mathbf{v} \times \mathbf{B}$ -axis

Small radial  
component,  
consistent with  
charge-excess  
component

Angle uncertainty:

$$\sigma \sim \frac{21^\circ}{\text{SNR}}$$



# Polarization results

- Charge-excess fraction on average 11 %, spread of distribution is 4 %.

Precision per air shower is about 2 %

- This depends on specific set of air showers, and on magnetic field and altitude of LOFAR
- Charge-excess fraction decreases with zenith angle, and increases with distance to shower axis, i.e. increases with opening angle from emission maximum

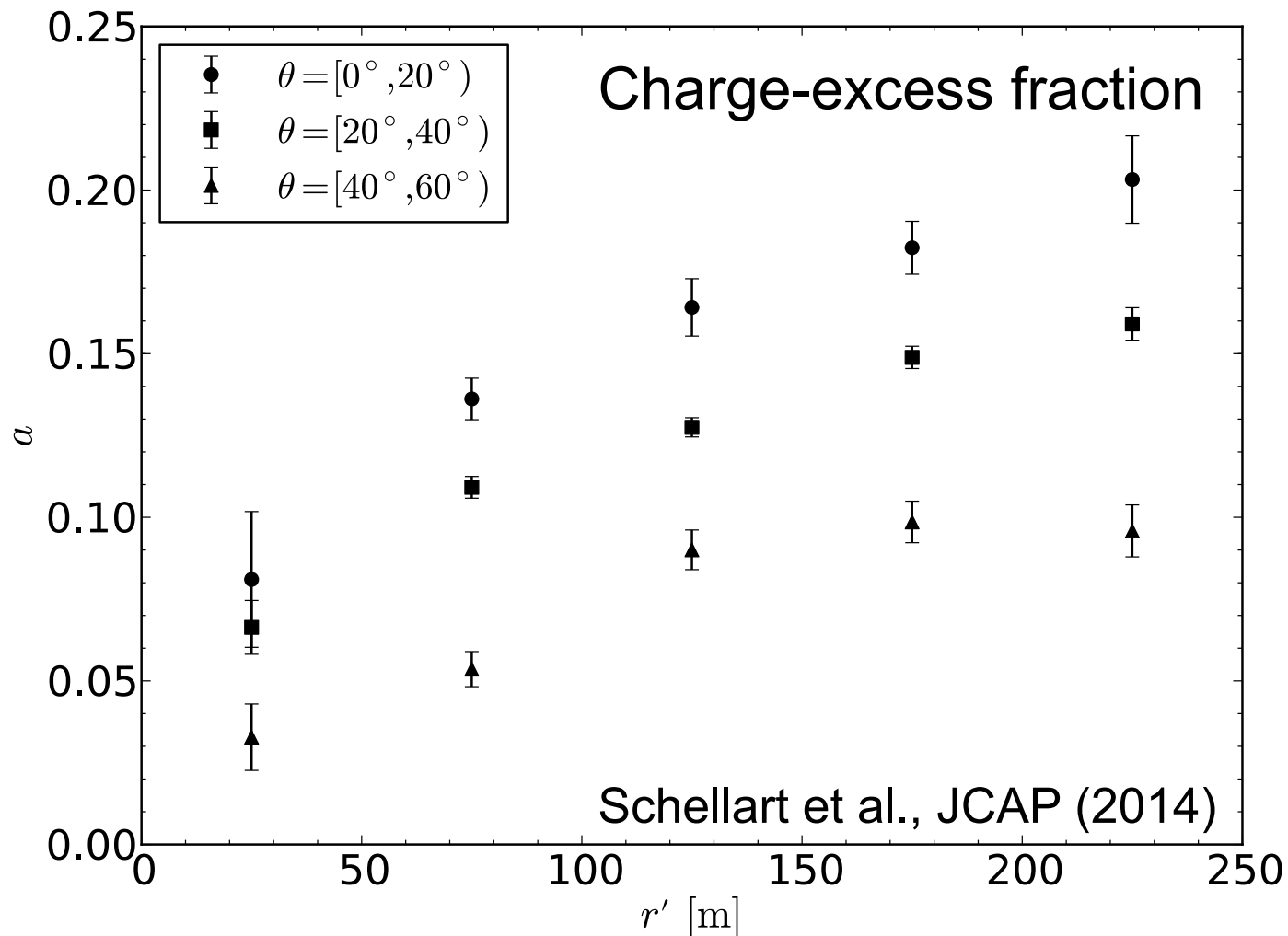


# Variations with zenith angle and distance to shower axis

Decreases with  
zenith angle

Increases with  
distance to  
shower axis

Agrees with  
expectations  
from theory  
and CoREAS  
(qualitatively)



# Conclusions

- With LOFAR, we have obtained high-precision measurements of polarization and radio wavefront shape
- Hyperbolic wavefront fits all cases, some of them also described by cone or parabola
- Polarization pattern well described by dominant geomagnetic contribution, and sub-dominant charge-excess component
- Qualitative agreement with theory and CoREAS simulations